

Nonlinear analysis and design of concrete-filled dual steel tubular columns under axial loading

Cheng-Yong Wan^a and Xiao-Xiong Zha^{*}

*Department of Civil and Environmental Engineering, Shenzhen Graduate School,
Harbin Institute of Technology, Shenzhen 518055, People's Republic of China*

(Received June 01, 2015, Revised August 05, 2015, Accepted November 18, 2015)

Abstract. A new unified design formula for calculating the composite compressive strength of the axially loaded circular concrete filled double steel tubular (CFDST) short and slender columns is presented in this paper. The formula is obtained from the analytic solution by using the limit equilibrium theory, the cylinder theory and the “Unified theory” under axial compression. Furthermore, the stability factor of CFDST slender columns is derived on the basis of the Perry-Robertson formula. This paper also reports the results of experiments and finite element analysis carried out on concrete filled double steel tubular columns, where the tested specimens include short and slender columns with different steel ratio and yield strength of inner tube; a new constitutive model for the concrete confined by both the outer and inner steel tube is proposed and incorporated in the finite element model developed. The comparisons among the finite element results, experimental results, and theoretical predictions show a good agreement in predicting the behavior and strength of the concrete filled steel tubular (CFST) columns with or without inner steel tubes. An important characteristic of the new formulas is that they provide a unified formulation for both the plain CFST and CFDST columns relating to the compressive strength or the stability bearing capacity and a set of design parameters.

Keywords: concrete filled double steel tube (CFDST); bearing capacity; unified formula; axial compression experiment; finite element analysis (FEA)

1. Introduction

With the uninterrupted development and application of steelwork industry in recent years, more and more concrete filled steel tubular frame structures are becoming a favourable choice in engineering practice provided that the issues of process, fabrication and welding are properly dealt with in column designs. To meet this requirement, various forms of cross-sectional structures are highly preferred. The advantages of concrete filled steel tubes (CFST) have been well recognized (Zhong 2006, Yu *et al.* 2013, Han *et al.* 2008, Eurocode 4 2004, Chinese Standard 2014).

As the application of engineering projects in combination with concrete filled steel tubular (CFST) columns such as industrial buildings, high-rise buildings, long-span bridges etc, the requirement of engineering structures of large-span, tower, heavy-load has been increased in recent

*Corresponding author, Professor, E-mail: zhahero@126.com

^a Ph.D. Student, E-mail: wanchengyong-2005@163.com

years. For large sectional scale of CFST members, there are inevitable problems in supplying, fabrication and welding of steel tubes, and also an effective confinement provided cannot be guaranteed. Moreover, creep effect is increased negatively in the circumstances of large sections. Much attention has been paid to overcoming the problem of large sectional scale for the use as compression members. As a result, some ideas were recommended in literature to reduce their dimensions; the following are some examples:

- (1) Filling the hollow steel tubes with reinforced concrete can develop the reinforced concrete filled steel tubular (RCFST) short columns (Xiamuxi and Hasegawa 2012, Wei *et al.* 2005). By doing so, the resulting columns are developed mainly for the purpose of combining the merits of RC and CFST structures.

Research results and application examples include the bearing capacity, toughness, ductility and anti-seismic performance of RCFST and CFST members. It was shown that the RCFST columns have good fire performance although they may not be as good as CFST columns in terms of strength. Fig. 1 shows the model form and application of RCFST for Shenzhen Jingji Financial Center of China.

- (2) To gain further benefit from the CFST columns, the concrete-filled double skin steel tubular (CFDSST) member has been proposed in recent years, which is a composite member consisting of an inner and outer steel skin with the annulus between the skins filled with concrete, as indicated in Fig. 1. Numerous research work has been done on this type of members in the past (Yagishita *et al.* 2000, Lin and Tsai 2001, Huang *et al.* 2010, Li *et al.* 2012), and it was found that the member inherited a similar behaviour from the CFST member. However CFDSST column may have a reasonable fire resistance period as its inner tube is protected by the sandwich concrete. An example for a real application of such kind of composite column is shown in Fig. 1, where concrete-filled double skin steel tubular columns serve as columns of transmission tower with high bending stiffness that avoids instability under outer pressure. During the construction or application, the sealing

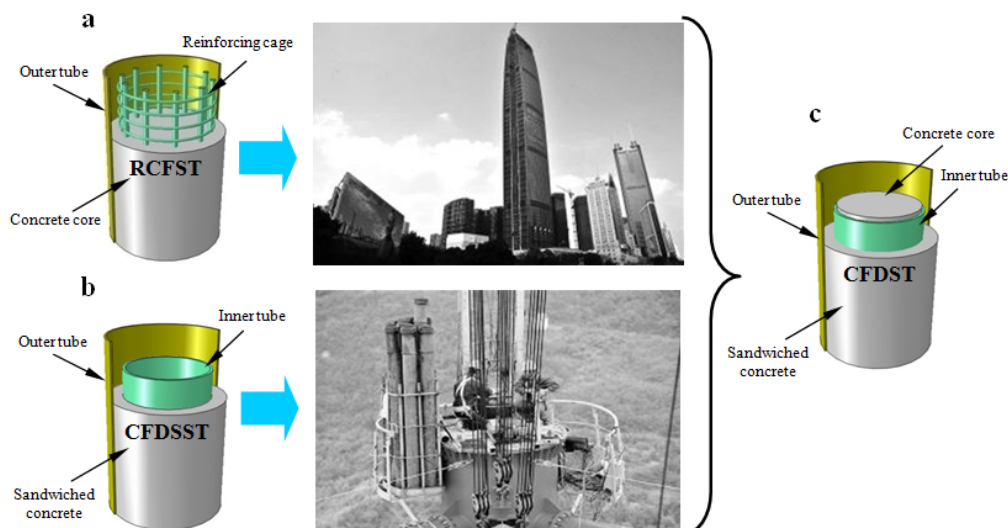


Fig. 1 Section form and application of composite columns. (a) Section form and application of RCFST column; (b) Section form and application of CFDSST column; (c) Section form of CFDSST column

property of the whole column cannot be guaranteed when there is a complicated and changeable environment as water vapor and air are likely to enter the hollow place as a result of hollow inner steel tube without core concrete. The destabilizing corrosion damage generated will affect the mechanical performance of CFDSST columns.

- (3) As illustrated in Fig. 1, this paper reports a new type of composite member, namely concrete filled double steel tubular (CFDST) column. This composite column consists of two concentrically placed steel tubes inside with concrete filled in both the double steel tubes. The CFDST column has a similar behaviour as the fully concrete filled steel tubular (CFST) column, such as simple section form, convenient construction and adequate bearing capacity. Compared with CFST members, the amount of the concrete can be reduced by the inner steel filling in it. Hence, the effective useful area can be increased, and a lighter self-weight can be obtained for the reduction of above 50% of the weight. CFDST member also has a better damping characteristic, ductility performance and reasonable fire resistance for the inner tubes are protected by the outer concrete. In some cases, it can be used to reinforce the existing CFST column for the goal of further improving the bearing capacity and the security of fire resistance. Besides, the ultimate axial strengths of CFDST column is much larger than that of CFST and CFDSST columns as it considers the concrete double confinement effects of the inner and outer layer of the steel tube.
- (4) More recently, a concrete filled stainless steel-carbon steel tubular column has been introduced as a new form of the composite member (Hassanein *et al.* 2013, Chang *et al.* 2013) which gives it the benefit of higher corrosion resistance and also combines the advantages of the stainless steel and the CFST columns as illustrated in Fig. 1(c). However, the expansive cost of the stainless steel is still the key factor which limits the extensive utilization of the members. For instance, the stainless steel is currently five times more expensive than carbon steel in China. Additionally, the iron and steel belong to the excess capacity industry nowadays in China, especially for the carbon steel with a low price. Hence, the concrete filled double steel tubular (CFDST) members adopting the carbon steel is reasonable in practice.

The above literature review indicates that there have been very limited studies (Chang *et al.* 2013, Liew and Xiong 2012, Jiang *et al.* 2008, Peng *et al.* 2011) on the behavior of circular concrete filled double steel tubular (CFDST) short columns and the research on CFDST slender columns has been reported only in the literature published by Romero *et al.* (2015) about the hollow steel tubular columns infilled with ultra-high strength concrete. This paper studies the ultimate axial strengths and behavior of circular concrete filled double steel tubular (CFDST) short and slender columns under axial loading. A new design formula of the ultimate axial strengths based on the CFST “Unified Theory” (Zhong 2006) is developed for CFDST columns under axial compression. This unified formula is not only in good agreement with that for CFST columns in predicting the behavior and strength of the columns with or without inner steel tube, but also consistent with the National code (Chinese Standard 2014). To demonstrate the proposed design formula, a series of compression tests were carried out on CFDST tubular short and slender columns, in which large-diameter-tube is used for short columns. Finally, as an attempt to give a further insight on the performance of the columns, a numerical analysis based on the general purpose finite element (FE) analysis program ABAQUS (ABAQUS standard 2008) was also conducted, and the new constitutive model of confined concrete has been greatly put forward.

2. Proposed new design strengths

2.1 Strength bearing capacity

The solution of axial compressive bearing capacity of the short CFDST column can employ limit equilibrium method (Гвоздев 1949), which does not consider the way of loading and deformation process. In order to get the limit condition of two components which is the steel tube and concrete, the bearing capacity of steel tube is obtained by Von Mises limit condition based on the thin-walled cylinder theory. It's considered to use the Lamé formula to solve the axial compressive strength of concrete under the thick-walled cylinder theory.

- (1) From the diameter to thickness ratio $D/t \geq 20$ of thin-walled steel tube, it can be found that the longitudinal stress σ_z and annular stress σ_θ are maintained to be uniform distribution along the wall, ignoring the radial stress σ_r . And the axial strength capacity of steel tube using Von Mises yield condition (such as Eq. (1)) can be derived

$$\sigma_z^{s2} + \sigma_z^s \sigma_\theta^s + \sigma_\theta^{s2} = f_s^2 \quad (1)$$

where σ_z^s is longitudinal stress of steel tube; σ_θ^s is annular stress of steel tube.

- (a) In order to deduce the longitudinal stress σ_{z1}^s of outer steel tube, first operating on this Eq. (1), leads to

$$\sigma_{z1}^s = \sqrt{f_s^2 - \frac{3}{4} \sigma_{\theta1}^{s2}} - \frac{\sigma_{\theta1}^s}{2} \quad (2)$$

where σ_{z1}^s is longitudinal stress of external steel tube; $\sigma_{\theta1}^s$ is annular stress of external steel tube.

To solve σ_{z1}^s , taking into account the mechanical analysis of half-sectional outer steel tube in Fig. 2(a) and the wall thickness of steel tube is small, and the mechanical equilibrium equation is obtained as follows

$$\sigma_{\theta1}^s (r_1 - r_2) = p_1 r_2 \quad (3)$$

$$A_s = 2\pi r_2 (r_1 - r_2), \quad A_c = \pi r_2^2 \quad (4)$$

Substituting Eqs. (3)-(4) into Eq. (2), leads to

$$\sigma_{z1}^s = \sqrt{f_s^2 - 3p_1^2 \left(\frac{A_c}{A_s}\right)^2} - \frac{p_1 A_c}{A_s} \quad (5)$$

- (b) In order to deduce the longitudinal stress σ_{z3}^s of inner steel tube, we first use the Eq. (1), which gives

$$\sigma_{z3}^s = \sqrt{f_s^2 - \frac{3}{4} \sigma_{\theta3}^{s2}} - \frac{\sigma_{\theta3}^s}{2} \quad (6)$$

in which σ_{z3}^s is longitudinal stress of internal steel tube; $\sigma_{\theta3}^s$ is annular stress of internal steel tube.

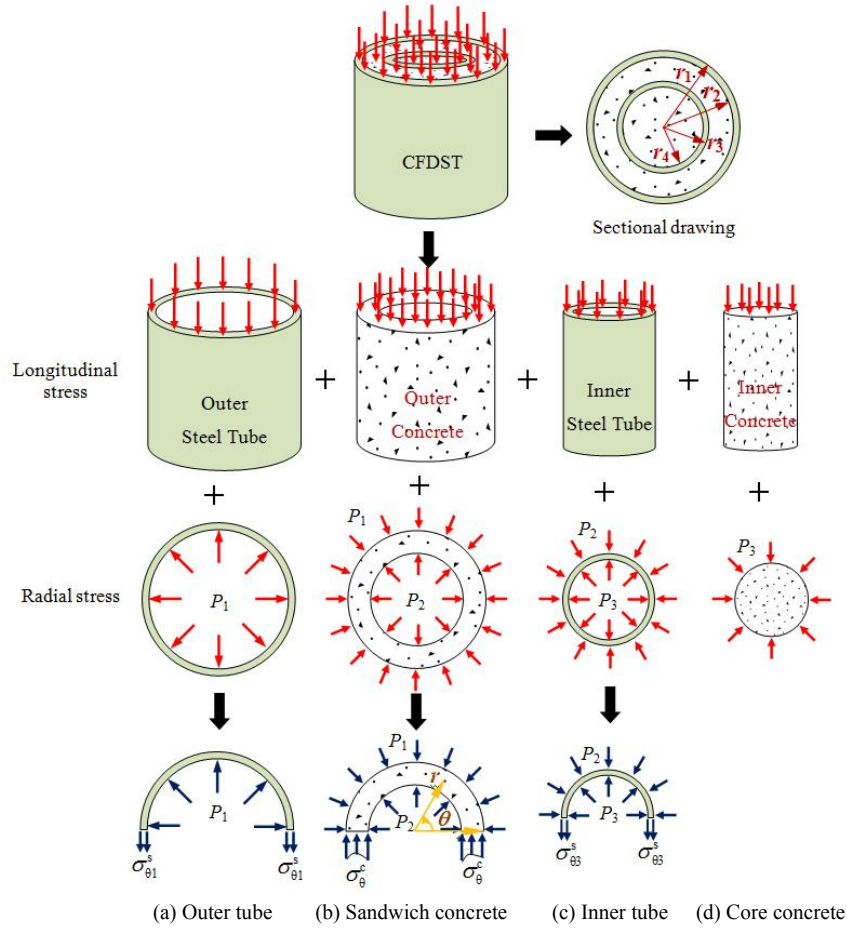


Fig. 2 The stress analysis diagram

Taking half-sectional steel tube to analysis of in Fig. 2(c) and considering the wall thickness of steel tube is small, and the mechanical equilibrium equation becomes

$$\sigma_{03}^s(r_3 - r_4) + p_2 r_3 = p_3 r_4 \tag{7}$$

$$A_{s,1} = 2\pi r_4 (r_3 - r_4) , \quad A_{c,2} = \pi r_4^2 \tag{8}$$

Substituting Eqs. (7)-(8) into Eq. (6), namely

$$\sigma_{z3}^s = \sqrt{f_s^2 - 3 \left[\frac{A_{c,2}(p_3 - p_2)}{A_{s,1}} \right]^2} - \frac{A_{c,2}(p_3 - p_2)}{A_{s,1}} \tag{9}$$

- (2) The axial compression strength of concrete consists of two parts, the contents of which are the strength bearing capacity σ_z^{c1} from Eq. (10) and σ_z^{c2} under axial force and lateral

pressure, respectively. And σ_z^c is obtained through the Lamé formulas, as shown in Eq. (11) below

$$\sigma_z^{c1} = -E_c \varepsilon_z^{sc} = -\sigma_c \quad (10)$$

$$\sigma_z^{c2} = \frac{2\nu_c}{r_2^2 - r_3^2} (r_3^2 p_2 - r_2^2 p_1) \quad (11)$$

$$\sigma_\theta^c = -\frac{r_2^2 r_3^2 (p_1 - p_2)}{r_2^2 - r_3^2} \frac{1}{r^2} + \frac{r_3^2 p_2 - r_2^2 p_1}{r_2^2 - r_3^2} \quad (12)$$

where σ_c is axial compressive strength of concrete; σ_θ^c is annular stress of concrete.

- (a) To solve longitudinal stress σ_{z2}^c of sandwich concrete, taking into account mechanical analysis of half-sectional sandwich concrete in Fig. 2(b), and the mechanical equilibrium equation is given below

$$2 \int_{r_3}^{r_2} \sigma_\theta^c dr - 2 \int_0^{\frac{\pi}{2}} p_1 \sin \theta d_2 d\theta + 2 \int_0^{\frac{\pi}{2}} p_2 \sin \theta d_3 d\theta = 0 \quad (13)$$

Substituting Eq. (12) into the above equation, and substituting Eq. (14) into Eq. (11), leads to

$$r_3 p_2 = r_2 p_1 \quad (14)$$

$$\sigma_{z2}^c = -\frac{2\nu_c r_2 p_1}{r_2 + r_3} \quad (15)$$

where σ_{z2}^c is longitudinal stress of sandwich concrete.

- (b) To solve longitudinal stress σ_{z4}^c of core concrete, referring to the above same procedure and conducting mechanical analysis on half-sectional core concrete in Fig. 2(d), leads to Eq. (16) as follows

$$\sigma_{z4}^c = -2\nu_c p_3 \quad (16)$$

where σ_{z4}^c is longitudinal stress of core concrete.

- (3) On the basis of the additive principle of limit equilibrium theory, the axial compressive bearing capacity design formula of the short CFDST column can be written as follows

$$N = A_{sc} \sigma_{sc} = A_s \sigma'_s + A_{c,1} \sigma'_{c,1} + A_{s,1} \sigma'_{s,1} + A_{c,2} \sigma'_{c,2} \quad (17)$$

$$\sigma'_s = \sigma_{z1}^s = \sqrt{f_s^2 - 3p_1^2 \left(\frac{A_c}{A_s}\right)^2} - \frac{p_1 A_c}{A_s} \quad (18)$$

$$\sigma'_{c,1} = \sigma_z^{c1} + \sigma_{z2}^c = -\sigma_c - \frac{2\nu_c r_2 p_1}{r_2 + r_3} \quad (19)$$

$$\sigma'_{s,1} = \sigma_{z3}^s = \sqrt{f_s^2 - 3\left[\frac{A_{c,2}(p_3 - p_2)}{A_{s,1}}\right]^2} - \frac{A_{c,2}(p_3 - p_2)}{A_{s,1}} \quad (20)$$

$$\sigma'_{c,2} = \sigma_z^{c1} + \sigma_{z4}^c = -\sigma_c - 2\nu_c p_3 \quad (21)$$

where σ'_s , $\sigma'_{s,1}$, $\sigma'_{c,1}$ and $\sigma'_{c,2}$ are the total axial stress of outer and inner steel tube with sandwich and core concrete, respectively.

Substituting Eqs. (18)-(21) into Eq. (17), it is clear that the axial strength analytical solution can be written as

$$\begin{aligned} \sigma_{sc} = & \left[\sqrt{\xi_1^2 - 3\left(\frac{p_1}{\sigma_c}\right)^2 (\beta_1 + \beta_2)^2} - \frac{p_1}{\sigma_c} (\beta_1 + \beta_2) \right] \sigma_c + \beta_1 \left[1 + \frac{1}{1 + \zeta_1} 2\nu_c \frac{p_1}{\sigma_c} \right] \sigma_c \\ & + \left[\sqrt{\xi_2^2 - 3\left(\frac{p_3 - p_2}{\sigma_c}\right)^2 \beta_2^2} - \frac{p_3 - p_2}{\sigma_c} \beta_2 \right] \sigma_c + \beta_2 \left[1 + 2\nu_c \frac{p_3}{\sigma_c} \right] \sigma_c \end{aligned} \quad (22)$$

$$\xi_1 = \frac{A_s \sigma_s}{A_{sc} \sigma_c}, \quad \xi_2 = \frac{A_{s,1} \sigma_{s,1}}{A_{sc} \sigma_c} \quad (23)$$

$$\beta_1 = \frac{r_2^2 - r_3^2}{r_1^2}, \quad \beta_2 = \frac{r_4^2}{r_1^2} \quad (24)$$

$$\zeta_1 = \frac{r_3}{r_2} \quad (25)$$

where ξ_1 , ξ_2 are the equivalent enhanced outer and inner tube confining coefficient, respectively; β_1 is the specific value of sandwich concrete sectional area and the whole area; β_2 is the specific value of core concrete sectional area and the whole area; ζ_1 is the relative diameter ratio between inner and outer steel tube.

Due to the greater size gap between the thickness ratio of inner and outer steel tube and the cross section external diameter, β_1 , β_2 can be approximately considered as

$$\beta_1 = \frac{r_2^2 - r_3^2}{r_2^2} = 1 - \zeta_1^2, \quad \beta_2 = \frac{r_3^2}{r_2^2} = \zeta_1^2 \quad (26)$$

Substituting Eq. (14) and Eq. (26) into Eq. (22), leads to

$$\begin{aligned} \sigma_{sc} = & \left[1 + \left(\sqrt{1 - \frac{3}{\xi_1^2} \left(\frac{\zeta_1 p_2}{\sigma_c} \right)^2} - \frac{\zeta_1 p_2}{\xi_1 \sigma_c} + (1 - \zeta_1) 2\nu_c \frac{\zeta_1 p_2}{\xi_1 \sigma_c} \right) \xi_1 \right. \\ & \left. + \left(\sqrt{1 - \frac{3}{\xi_2^2} \left(\frac{p_3 - p_2}{\sigma_c} \right)^2 \zeta_1^4} - \frac{p_3 - p_2}{\xi_2 \sigma_c} \zeta_1^2 + \zeta_1^2 2\nu_c \frac{p_3}{\xi_2 \sigma_c} \right) \xi_2 \right] \sigma_c \end{aligned} \quad (27)$$

To obtain the maximum strength bearing capacity, it is necessary to derive the Eq. (27) with respect to P_2 and P_3 , and the lateral pressure p_2^* and p_3^* as the following can be gained through the limit condition (as shown in Eq. (28)) where σ_c is the maximum value, besides $\sigma_c = f_{ck}$, $\sigma_{sc} = f_{sc}$.

$$\frac{d\sigma_{sc}}{dp_2} = 0, \quad \frac{d\sigma_{sc}}{dp_3} = 0 \quad (28)$$

$$\frac{p_2^*}{\sigma_c} = \frac{(2\nu_c - 1)\xi_1}{\zeta_1 \sqrt{12(\nu_c^2 - \nu_c + 1)}} \quad (29)$$

$$\frac{p_3^*}{\sigma_c} = \frac{(2\nu_c - 1)(\xi_2 + \zeta_1 \xi_1)}{\zeta_1^2 \sqrt{12(\nu_c^2 - \nu_c + 1)}} \quad (30)$$

Substituting Eqs. (29)-(30) into Eq. (27), becomes

$$f_{sc} = [1 + (\sqrt{1 - 3(\frac{(2\nu_c - 1)}{\sqrt{12(\nu_c^2 - \nu_c + 1)}})^2} - \frac{(2\nu_c - 1)}{\sqrt{12(\nu_c^2 - \nu_c + 1)}} + \frac{(1 - \zeta_1)2\nu_c(2\nu_c - 1)}{\sqrt{12(\nu_c^2 - \nu_c + 1)}})\xi_1 + (\sqrt{1 - 3(\frac{(2\nu_c - 1)}{\sqrt{12(\nu_c^2 - \nu_c + 1)}})^2} - \frac{(2\nu_c - 1)}{\sqrt{12(\nu_c^2 - \nu_c + 1)}} + \frac{2\nu_c(2\nu_c - 1)(\xi_2 + \zeta_1 \xi_1)}{\zeta_1^2 \sqrt{12(\nu_c^2 - \nu_c + 1)}})\xi_2] f_{ck} \quad (31)$$

The above formula should be simplified as

$$f_{sc} = [1 + (\sqrt{1 - \frac{(2\nu_c - 1)^2}{4(\nu_c^2 - \nu_c + 1)}} + \frac{(2\nu_c - 1)^2}{\sqrt{12(\nu_c^2 - \nu_c + 1)}})\xi_1 + (\sqrt{1 - \frac{(2\nu_c - 1)^2}{4(\nu_c^2 - \nu_c + 1)}} + \frac{(2\nu_c - 1)^2}{\sqrt{12(\nu_c^2 - \nu_c + 1)}})\xi_2] f_{ck} \quad (32)$$

namely

$$f_{sc} = [1 + \alpha(\xi_1 + \xi_2)] f_{ck} \quad (33)$$

thus calculation formula of the axial compressive bearing capacity of CFDST short column can be solved below as

$$N = f_{sc} A_{sc} = [1 + \alpha(\xi_1 + \xi_2)] f_{ck} A_{sc} \quad (34)$$

in which α must be treated as an impact factor in connection with the Poisson's ratio of concrete.

From the above derived process (as shown in Eq. (34)), it is clear that the axial compressive bearing capacity has nothing to do with the relative position of the steel tube inside and outside, but is related to the Poisson's ratio of concrete, this holds as long as the internal equal area of the steel tube, and the strength capacity value is the same. The "Unified theory" (Zhong 2006) is then introduced to derive the bearing capacity formula, which uses the assumption that the concrete-filled steel tube is regarded as a unified body, which is a composite material, and its behavior changes with the change in the physical parameters of the materials, the geometrical parameters of the members, the types of cross-sections and the stresses states. Considering the combined confining coefficient ζ^* , the formula for calculating the ultimate bearing capacity is then given by

$$N = f_{sc} A_{sc} = [1 + k \xi^*] f_{ck} A_{sc} \quad (35)$$

$$\xi^* = \frac{A_s f + A_{s,1} f_{s,1}}{A_c f_{ck}} \quad (36)$$

where k is the influence coefficient; $f, f_{s,1}$ are yield strength of outer and inner steel tube, respectively.

In accordance with relevant regulations of the current national standard (Chinese standard 2014), on the basis of the common CFST column, the simplified bearing capacity unified formula of CFDST column can be gained, as shown in Eq. (37).

$$N = (1.212 + B \xi^* + C \xi^{*2}) f_{ck} A_{sc} \quad (37)$$

$$B = \left(\frac{0.176 \times f}{235} + 0.974 \right) \quad (38)$$

$$C = \left(\frac{-0.104 \times f_{ck}}{20.1} + 0.031 \right) \quad (39)$$

where B and C are the coefficients depending on the cross-sectional geometry.

For a concrete filled multilayered steel tube, based on Eq. (37), the unified formula for the axial compressive bearing capacity through not the considering the influence of the relative position of internal and external steel tube can be written as Eq. (40) shown as follow

$$N = (1.212 + B \xi_i^* + C \xi_i^{*2}) f_{ck} A_{sc} \quad (40)$$

$$\xi_i^* = \frac{A_s f + \sum_{i=1}^n A_{s,i} f_{s,i}}{A_c f_{ck}} \quad (41)$$

where ξ_i^* is the enhanced equivalent confining coefficient for circular section with i layers steel tube inside; $A_{s,i}, f_{s,i}$ are the cross-sectional area and yield strength of the i layers steel tube inside, respectively.

2.2 Stability bearing capacity

The above approach for developing the unified strength formula also applies to the formulation of the stability factor of the slender CFDST columns. By considering a concrete-filled double steel tube column as a column made of a composite material, the stability factor can be obtained from Perry-Robertson formula. The fundamental assumption is that regardless of the effect of residual stress, the yield load can be calculated when the edge fibre yield of the central section happens

under the effect of the second-order bending moment $\frac{Nf_0}{1 - N/N_E}$ produced by the initial bending as the main initial geometric imperfection. Thus, the yield stress σ_T is given by

$$\sigma_T = \frac{N}{A} + \frac{Nf_0}{W(1-N/N_E)} \quad (42)$$

It is assumed that

$$\sigma_e = \frac{N_E}{A}, \quad \sigma_0 = \frac{N}{A}, \quad \varepsilon = \frac{Af_0}{W} \quad (43)$$

where, A , W are the sectional area and bending modulus of the members, respectively; f_0 is the initial bending of the vector height; σ_0 , σ_e denote the mean stress and Euler stress of the material, respectively; ε is the initial eccentricity and $\varepsilon > 0$.

Substituting Eq. (43) into Eq. (42) and using some simplification, it yields

$$\sigma_0^2 - \sigma_0[\sigma_T + \sigma_e(1+\varepsilon)] + \sigma_e\sigma_T = 0 \quad (44)$$

When σ_0 is regarded as critical stress of the edge fibre yield criterion, the stability factor is defined as

$$\varphi = \sigma_0 / \sigma_T \quad (45)$$

An alternative form of Perry-Robertson formula through substituting Eq. (44) into Eq. (45) yields

$$\varphi = \frac{1+(1+\varepsilon)\frac{\sigma_e}{\sigma_T}}{2} - \sqrt{\left(\frac{1+(1+\varepsilon)\frac{\sigma_e}{\sigma_T}}{2}\right)^2 - \frac{\sigma_e}{\sigma_T}} \quad (46)$$

For a concrete-filled double steel tube that is assumed as a composite unit, $\sigma_T = f_{sc}^*$, and the Euler stress can be expressed as $\sigma_{esc} = \frac{\pi^2}{\lambda^2} E_{sc}$. The non-dimensional slenderness is then defined as

$$\overline{\lambda}_{sc} = \frac{\lambda}{\pi} \sqrt{\frac{f_{sc}^*}{E_{sc}}} \quad (47)$$

where the slender ratio $\lambda = L_0 / i_{sc}$, L_0 is the effective length of the column, gyration radius $i_{sc} = \sqrt{I_{sc} / A_{sc}}$; f_{sc}^* is the equivalent compressive strength, namely

$$f_{sc}^* = \frac{N}{A_{sc}} \quad (48)$$

and E_{sc} is the composite bending modulus of CFDST, given by

$$E_{sc} = \frac{E_{is}I_{is} + E_{os}I_{os} + E_cI_c}{I_{sc}} \quad (49)$$

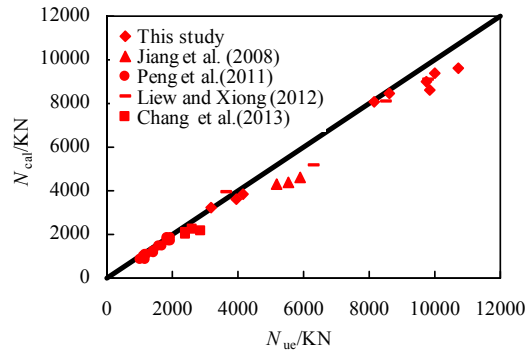


Fig. 3 Comparisons of axial capacity between the design solutions and the experimental results

where E_{os}, E_{is}, E_c are the elastic modulus of outer, inner steel tube and concrete, respectively; I_{os}, I_{is}, I_c are the moments of inertia of outer, inner steel tube and concrete, respectively.

From the above analysis, the unified formulation for predicting the axial load bearing capacity of the long circular CFDST columns can be expressed as follows

$$N_u = \varphi N \tag{50}$$

$$\varphi = \frac{1}{2\lambda_{sc}^2} \left[\lambda_{sc}^{-2} + (1 + K\lambda_{sc}) - \sqrt{(\lambda_{sc}^{-2} + (1 + K\lambda_{sc}))^2 - 4\lambda_{sc}^{-2}} \right] \tag{51}$$

where $K=0.25$ is the equivalent relative initial flexural factor recommended by Ref. (Yu *et al.* 2013).

In order to verify the effectiveness of the unified formula of the stability bearing capacity of the concrete-filled double steel tubular columns under axial compression, comparisons are made between the design solutions and the experimental results for the slender columns. A mean (N_{cal}/N_{ue}) of 0.890 and a variance of 0.005 are obtained, which are given in Fig. 3. Good agreement is evident.

3. Experimental programme

3.1 Specimen design

For each tested specimen, both tubes were first welded on an end plate concentrically, followed by the concrete casting, and then the other ends of the tubes were welded to another end plate. A total of 10 specimens were tested including 7 CFDST and 1 CFST short columns, 2 CFDST and 1 CFST slender columns. The two CFST specimens were taken as references. Table 1 lists the details of the specimens, where D_o and D_i are the outer and inner diameters of circular hollow section (CHS), respectively; t_o and t_i are the thicknesses of the outer and inner tubes, respectively; and L is the height of the specimen. The experimental parameters include the steel ratio ρ_i and yield strength f_{yi} of the inner tube. The steel ratios ρ_i of the inner tube are 1.81%, 3.04% and 3.81%, respectively, and for the slender columns, ρ_i are 2.00% and 3.04%, respectively, where ρ_i is defined

as A_i/A_{ce} . All tested specimens were labeled so that the types of columns, inside the tubular diameter and the strength can be easily identified. The comparative values of experimental results and the theoretical results from the above derived formulas are listed in Table 1.

3.2 Materials properties

The strength grade of concrete is designed as C30. With the purpose of determining the compressive strength of concrete, four groups of concrete test cubes are fabricated and cured in the same condition as the specimens, where each group includes three test cubes. The average concrete cube strength of each group is tested after 28 days, with the first day taken as the day when the experiment begins, on the day as the half of experiment has been finished and on the last day as the whole experiment finishes, respectively. Based on the above four groups of the average concrete strength, it is found that they have little difference. Thus, the cube compressive strength f_{cu} is determined as the mean value of the latter three groups of strength values, as shown in Table 1. The properties of steel used for tube specimens were determined by standard tensile coupon tests in accordance with the Chinese Standard GB/T 229.1 (2010). Three coupons were taken from each kind of steel tube. For the outer steel tube, Q275B is adopted, and the elastic modulus is 206 GPa. For the inner tube, Q345 and Q460 are used and the corresponding elastic modulus is 200 GPa. The Poisson's ratio μ_s for inner and outer steel is 0.3. The detailed properties of steel tube are given in Tables 2-3.

Table 1 Summary of experimental research on CFDST columns

Specimen ID	D_o /mm	t_o /mm	D_i /mm	t_i /mm	L /mm	f_{yo} /MPa	f_{yi} /MPa	f_{cu} /MPa	N_{cal} /kN	N_{fe} /kN	N_{ue} /kN	$\frac{N_{cal}}{N_{ue}}$	$\frac{N_{fe}}{N_{ue}}$
A-1	426	7.78	—	—	1300	313	—	30.51	7223	7054	6826	1.058	1.033
A1-1	426	7.73	133	6.6	1300	298	331.4	30.51	8101	8233	8142	0.995	1.011
A2-1	426	7.52	133	6.6	1300	302	460	30.51	8633	8865	9830	0.878	0.902
A1-2	426	7.52	219	6.7	1300	302	316.8	30.51	8633	8865	9830	0.878	0.902
A2-2	426	7.52	219	6.7	1300	302	478	30.51	9359	9648	10025	0.934	0.962
A1-3	426	7.52	273	6.5	1300	302	322	30.51	8976	9401	9740	0.922	0.965
A2-3	426	7.52	273	6.5	1300	302	447	30.51	9649	10156	10739	0.899	0.946
B-1	273	6.81	—	—	3300	328	—	30.51	3243	3070	3155	1.028	0.973
B1-1	273	6.86	89	4.7	3300	328	357.1	30.51	3652	3593	3924	0.931	0.916
B1-2	273	6.81	133	5	3300	328	331.8	30.51	3813	3780	4163	0.916	0.908

Table 2 Material properties of outer steel tube

Group	Type	t_o /mm	f_{yo} /MPa	f_{so} /MPa	E_{os} /MPa
Short column	Q275B	7.52	302	407	2.06×10^5
	Q275B	7.73	298	408	2.06×10^5
	Q275B	7.78	313	437	2.06×10^5
Slender column	Q275B	6.86	328	430	2.06×10^5
	Q275B	6.81	328	430	2.06×10^5

Table 3 Material properties of inner steel tube

Group	Type	D_i /mm	f_{yi} /MPa	f_{si} /MPa	E_{is} /MPa
Short column	Q345	133	331.4	478	2.0×10^5
	Q345	219	316.8	460	2.0×10^5
	Q345	273	322	415	2.0×10^5
	Q460	133	460	683	2.0×10^5
	Q460	219	478	660	2.0×10^5
	Q460	273	447	626	2.0×10^5
Slender column	Q345	89	357.1	490	2.0×10^5
	Q345	133	331.8	461	2.0×10^5

3.3 Test setups and instrumentation

A hydraulic testing machine of 15000 kN capacity is used to apply the axial compressive force to the column specimens with both ends of steel support. As shown in Fig. 4(c), twelve and twenty strain gauges are used for each specimen to measure the longitudinal and circumferential strains at the mid-height of the short and slender columns, respectively. Three longitudinal mechanical dial gauges with the label “1”, “2” and “3” are used to measure the axial displacement of the short columns; two radial dial gauges at the mid-height section with the label “4” and “5” are utilized to determine the roughness and deformation of steel tube on both sides of the short columns in the process of loading (see Fig. 4(a)). As shown in Fig. 4(b), the slender columns have four longitudinal mechanical dial gauges with the label “6”, “7” and “8”, “9”, in which two dial gauges with the label “6” and “7” are employed to measure the axial displacement of the columns, and the dial gauges of the label “8” and “9” are utilized to determine the direction of flexural deformation of the whole slender column.

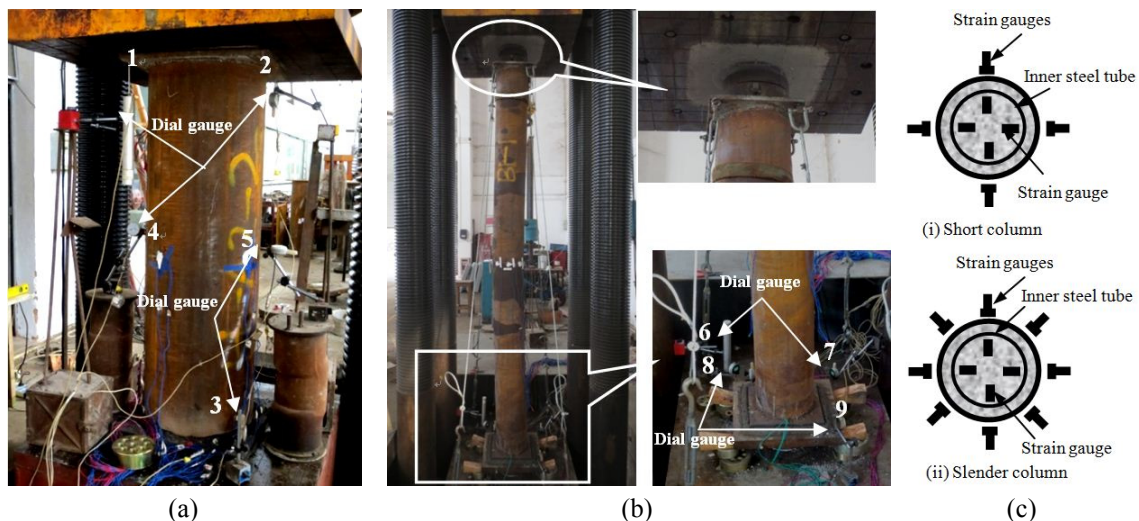


Fig. 4 Test set-up and instrumentation. (a) Short CFDST column during loading; (b) Slender CFDST column during loading; (c) Arrangement form of strain gauges with inner and outer steel tube

The test is conducted by electro-hydraulic servo control system. Each specimen is preloaded to the 20% of the theoretical bearing capacity before loading for the sake of checking whether the test devices and measuring instruments are normal working or not, adjusting positioning leveling of the columns and eliminating the influence of virtual displacement. At the initial stage of loading, the load is applied at a small speed of 4 kN/s until the strain value reaches 0.002 approximately. Then, the displacement control is adopted and loading speed is 0.035 mm/s until the descending period of displacement-load curve decreases by 30% of ultimate load. When the loading process maintains load control, each load interval is maintained for about 2 minutes. At each load or displacement increment generated by diverse loading ways the strain readings and the deflection measurements are recorded. An illustration of the test is shown in Fig. 4.

3.4 Phenomenon and failure modes

The specimens behaved in a ductile manner during the test greatly. Fig. 5 shows the typical overall failure modes of all the specimens after the test. It can be seen from Figs. 5(a)-(b) that, for the short CFDST columns, the whole specimen appears staggered vertical Luders-sliding-lines with the angle of 45° , where Luders-sliding-line is a surface line marking on a metal (as steel tube) caused by localized plastic deformation or flow of the material strained beyond its elastic limit. As the load increases, the outward buckling of outer steel tube occurs near the position of the bottom

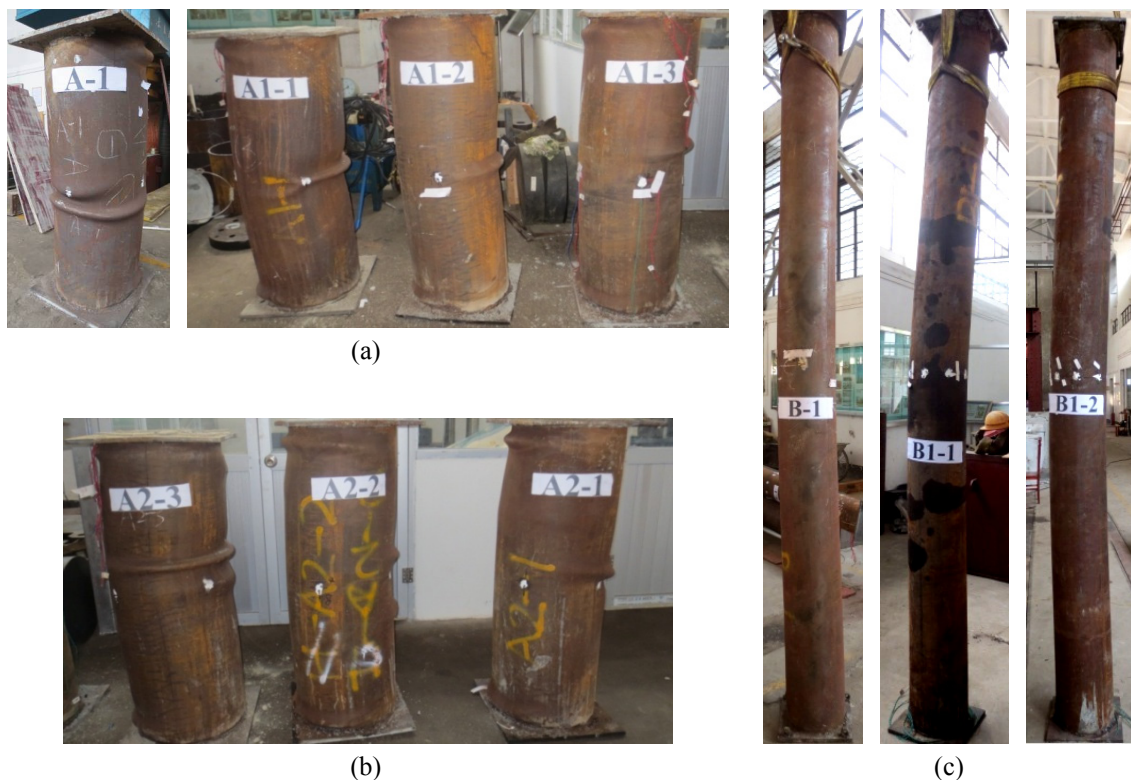


Fig. 5 Failure modes of specimens. (a) Grade Q345 in short column; (b) Grade Q460 in short column, (c) Grade Q345 in slender column

and top and middle-height end, respectively. While the direction of the buckling between the central and the top-bottom parts is opposite, which is due to the interaction between the steel tube and concrete. For the slender CFDST columns, with the great influence of initial eccentricity and defect, the specimens appear unstable failure as the same as compression-bending failure. The greater lateral deformation laid on the middle-height section, and there is a small amount of slipping line in the central position of outer surface of the steel tube, as shown in Fig. 5(c).

After the test, the outer steel tube was removed and the failure modes of sandwiched and core concrete with inner tube are shown in Fig. 6. It can be seen from the figure that, for the label A2-2 of the typical short column, the concrete was crushed at the top and middle-height sections where the outward buckling occurred. Meanwhile, in spite of the support of the sandwiched and core concrete, obvious outward buckling and deformation was found in the inner tube, which declares that steel tube had attained yield strength and stepped into the stage of plastic flow, as shown in Fig. 6(c). For the inner core concrete, owing to the larger bearing capacity and sectional size, the frictional tendency between coverplate and loading surface enhances and shear force presents heighten. Thus, the failure of core concrete appears shear failure mode. But as a result of the collaborative work and constraint from the inner tube, the shear capacity is improved, as shown in Fig. 6(d). In general, the column with a small diameter will not have this kind of failure mode. Figs. 6(e)-(f) illustrated the failure mode of the typical slender column as label B1-1. It can be seen that this failure mode of the inner concrete and steel tube was also similar to that of the circular CFST columns. Furthermore, no crack or slip was observed on the interfaces between the tubes and the sandwiched and core concrete except the failure zone. It can be concluded that the concrete and steel tubes can work together well despite the slender ratio.

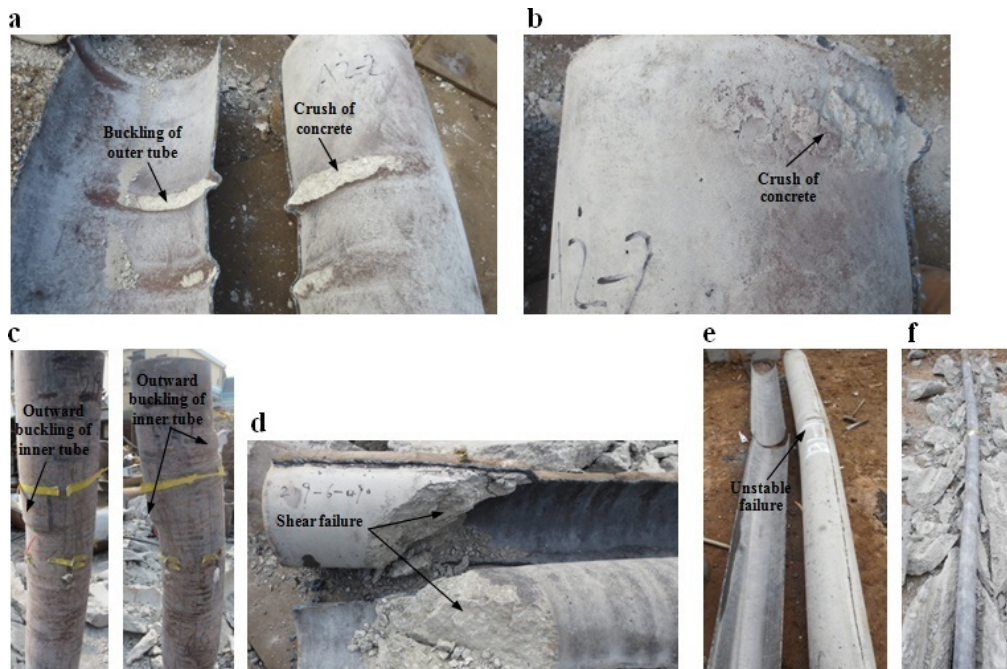


Fig. 6 Typical failure mode of specimens after split. (a) Crush of concrete at the middle-height sections; (b) Crush of concrete at the top sections; (c) Buckling of inner tube; (d) Shear failure of core concrete; (e) Failure mode of slender column; (f) Failure mode of inner tube

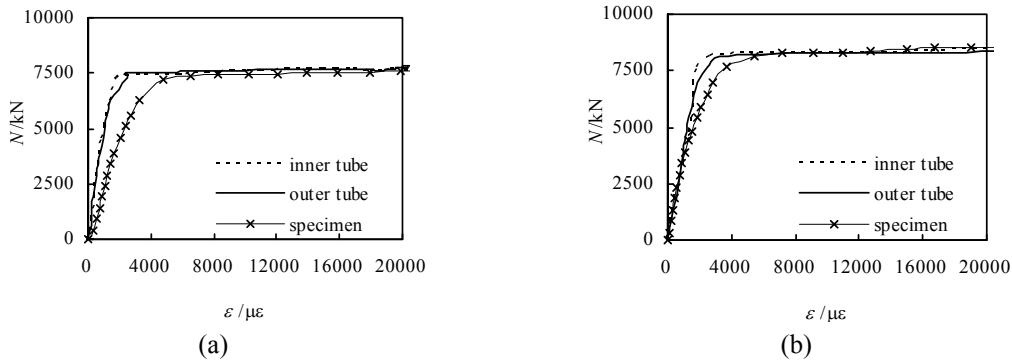


Fig. 7 Typical load(N) versus strain (ε) curves of specimens. (a) Specimen A1-1; (b) Specimen A2-1

3.5 Full curves of load-deformation

The typical load-strain relationship curves are measured for short column specimens of label as A1-1 and A2-1 in Fig. 7, where the equivalent strain for the entire column is defined as the whole measured axial compressive displacement value u divided by the height L of the column, and it also gives load-strain curves of inner and outer steel tubes, where the specimen A1-1 and A2-1 have the same dimension and material parameters except the yield strength of the inner steel tube. It is clear that the strain development curve changing law is similar between the inner and outer tube. Before reaching the ultimate load, the inner and outer steel tubes have yielded, in which the steel tubes exert their compressive strength and double confinement effect on the core concrete. With the same steel tube ratio, the higher inner tube yield strength leads to more obvious double confinement effect, which can improve the ultimate load further.

The influence of the inner steel ratio on the load-displacement for short column specimens is illustrated in Figs. 8(a)-(b), where all specimens have the same dimension and material parameters except the inner steel ratio with 0, 1.81%, 3.04% and 3.81%, respectively. It is clear that the greater inner steel ratio gives rise to higher column strength. For the slender column specimens, Fig. 8(c) shows the load-strain relationship curves measured with the inner steel ratio of 0, 2.00% and 3.04%, respectively. It can be seen that increasing the steel ratio significantly increases the

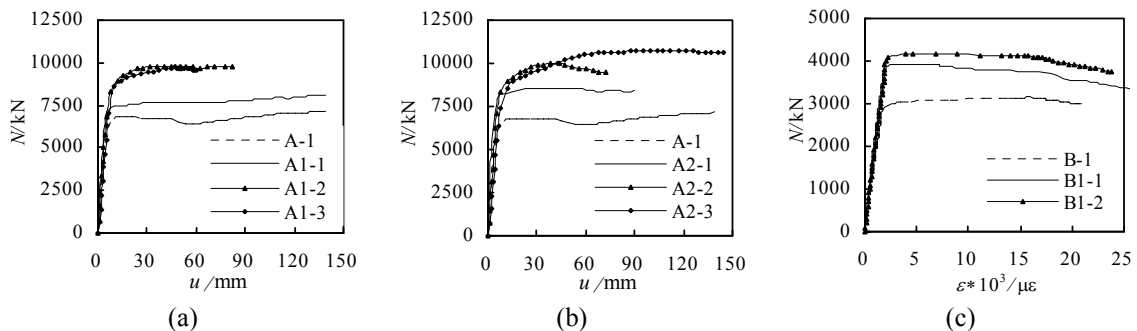


Fig. 8 Influence on load versus displacement curves with steel ratio. (a) Grade Q345 in short column; (b) Grade Q460 in short column; (c) Grade Q345 in slender column

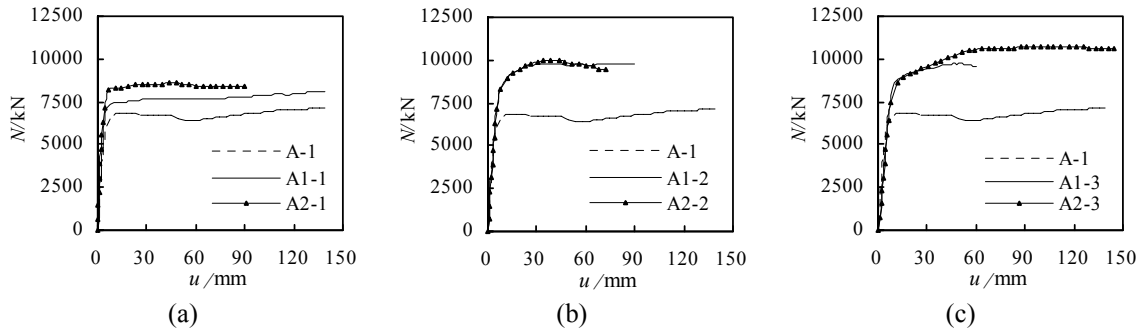


Fig. 9 Influence on load versus displacement curves with inner steel strength.
 (a) $\rho = 1.81\%$; (b) $\rho = 3.04\%$; (c) $\rho = 3.81\%$

ultimate axial strength of the circular CFDST columns. Moreover, the slender CFDST columns exhibit large axial strains without failure, having very good ductility.

The acquired axial load-displacement curves for the current CFDST columns can be classified into three types as shown in Fig. 9, where the inner steel tube yield strength is divided as grade Q345 and Q460. Clearly, it can be noticed that increasing the f_{yi} value of the inner steel tube, for the same steel ratio ρ_i , results in an increase in the strength of the CFDST column. And the setup of inner steel tube, the gained axial compressive stiffness is larger than that of the conventional concrete filled steel tubular column. While the steel ratio reached a certain limit value, the improvement in the strength is not obvious. Since the steel tube inside can improve the bearing capacity and stiffness of the frame column, reducing additional bending moment *et al.* caused by the axial displacement is of great significance.

4. Finite element analysis

In order to further understand the behaviors of the composite columns reported in the previous sections, the finite element analysis using ABAQUS was conducted. This method is often used in static analysis and shows to be efficient for nonlinear analysis. The material nonlinearities of concrete and steel tubes as well as the concrete confinement were considered in the analysis. The details of the FE model used for CFDST columns are described in the following sections.

4.1 Model description

4.1.1 Constitutive models

The structural behaviour of CFDST columns depends on the mechanical properties of steel. Carbon steel is assumed to behave as elastic-plastic materials with strain hardening after yield strength. The response of the steel tube is modeled by an elastic-plastic theory with the Von-Mises yield criteria, associated with the flow rule and isotropic strain hardening. The bilinear elastic-plastic stress-strain curve with linear strain hardening used to simulate the steel material is shown in Fig. 10(a). When the stress points fall inside the yield surface, the behavior of the steel tube is linearly elastic, where the Young's modulus of $E_s = 206$ GPa and Poisson's ratio of $\mu_s = 0.3$ were used. If the stresses of steel tube reach the yield surface, in the hardening part of the curve, a modulus of 2 GPa was used, and the behavior of the steel tube becomes perfectly plastic.

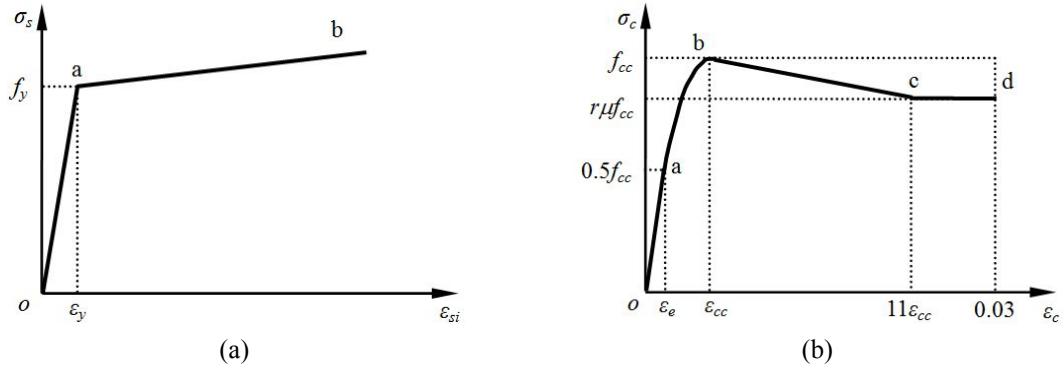


Fig. 10 Stress-strain curve in circular CFDST columns. (a) Bilinear stress-strain curve of steel; (b) Stress-strain curve for confined concrete

Since steel tubes can provide confining effect on concrete core in CFDST columns, equivalent uniaxial stress-strain relationship for confined concrete should be adopted. Fig. 10(b) shows the general stress-strain curve to simulate the material behaviour of confined concrete. The first part *oa* of the stress-strain curve is the initially assumed elastic range to the proportional limit stress and the curve depicted is represented by

$$\sigma_c = 0.5f_{cc} \frac{\varepsilon_c}{\varepsilon_e} \quad \varepsilon_c < \varepsilon_e \quad (52)$$

where σ_c is the longitudinal compressive concrete stress, ε_c is the corresponding strain at σ_c . The value of the proportional limit stress is taken as $0.5f_{cc}$ as given by Richart *et al.* (1928), and ε_e is the corresponding proportional limit strain calculated by Eq. (54). Besides, f_{cc} is the compressive cylinder strength of the confined concrete converted from cube strength (f_{cu}) which is equal to $0.8f_{cu}$.

While the initial Young's modulus of confined concrete (E_{cc}) is reasonably calculated using the empirical Eq. (53) given by ACI (2002). The Poisson's ratio (μ_{cc}) of concrete under uniaxial compressive stress ranges from 0.15 to 0.22. In this study, the Poisson's ratio of concrete is assumed to be $\mu_{cc} = 0.2$

$$E_{cc} = 4730\sqrt{f_{cc}} \quad (53)$$

The stress-strain relationship model proposed by Saenz (1964) was widely accepted as the second part *ab* of the uniaxial stress-strain curve for the concrete. It has the following form

$$\sigma_c = \frac{E_c \varepsilon_c}{1 + R_2(R_1 + R_E - 2) - (2R_1 - 1)(R_2)^2 + R_1(R_2)^3} \quad \varepsilon_e \leq \varepsilon_c < \varepsilon_{cc} \quad (54)$$

where R_1 , R_2 and R_E values are calculated from Eq. (55), respectively

$$R_1 = \frac{R_E(R_\sigma - 1)}{(R_E - 1)^2} - \frac{1}{R_E}, \quad R_2 = \frac{\varepsilon_c}{\varepsilon_{cc}}, \quad R_E = \frac{E_c \varepsilon_{cc}}{f_{cc}} \quad (55)$$

R_σ and R_E are determined as

$$R_\sigma = R_\epsilon = 4 \tag{56}$$

The confined concrete compressive strength (f_{cc}) and the corresponding confined strain (ϵ_{cc}) can be determined using the strength reduction factor r_c (Liang 2009) from Eqs. (57)-(58), respectively, based on the work of Mander *et al.* (1988).

$$f_{cc} = r_c f_c + k_1 f_{cl} \tag{57}$$

$$\epsilon_{cc} = \epsilon_c \left(1 + k_2 \frac{f_{cl}}{r_c f_c} \right) \tag{58}$$

where k_1 and k_2 is constants and suggested to be 4.1 and 20.5, according to the studies conducted by Richart *et al.* (1928). f_c is the unconfined compressive cylinder strength of concrete and ϵ_c is the corresponding strain at f_c , and the value of ϵ_c is usually around the range of 0.002 to 0.003. A representative value of ϵ_c is taken as 0.002 in this analysis. The value of f_{cl} having significant effect for steel tube can be determined by the empirical formulas proposed in this paper.

Experiments indicated that the effective compressive strength of concrete varies from $0.8 f_c$ to $1.0 f_c$ (Martinez 1984). Generally, the larger the section diameter is, the smaller the corresponding concrete strength. Thus, r_c is defined as the strength reduction factor that accounts for the size effect, the quality of concrete and the loading rates on the concrete compressive strength. The equation of circular plain concrete columns by Sakino *et al.* (2004) is modified by taking into account the influence of the formwork here. As shown in Fig. 11, a comparison of the previous strength reduction factor and the proposed r_c has been given, and the strength reduction factor for compressed concrete is proposed as

$$r_c = 1.75 D_c^{-0.123} \tag{59}$$

where D_c is the nominal diameter of the circular concrete core and taken as value of $(D_o - 2t_o)$. It is found that the proposed r_c is conservative compared to the strength reduction factor given by Sakino *et al.* (2004) as a result of the uncertainty of the interface between concrete and steel tube.

When $\epsilon_{cc} \leq \epsilon_c < 11\epsilon_{ci}$, a linear descending line is used to model the softening behavior of concrete as shown in Fig. 10. The third part bc is also assumed to start from the confined strength f_{cc} and end at $\epsilon_c = r\mu f_{cc}$. The corresponding strain was formulated as $\epsilon_c = 11\epsilon_{cc}$. The straight line of

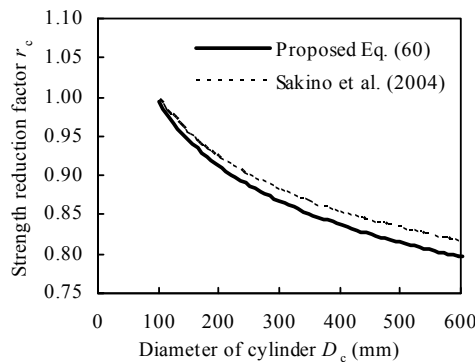


Fig. 11 Scale effect on compressive strength of circular concrete column

the fourth part cd is depicted to be terminated at the point where $\varepsilon_c = r\mu f_{cc}$ and $\varepsilon_c = 0.03$. If the value of $11\varepsilon_{cc}$ is larger than or equal to 0.03 with the corresponding stress of $r\mu f_{cc}$, it is assumed as $11\varepsilon_{cc}$ identically equal to 0.03. Meanwhile, the quadri-polygonal line of the relationship curve has to be identified as the three parts. The parts bc and cd of the stress-strain curve are represented by

$$\sigma_c = \begin{cases} [11 - R_2 - (1 - R_2)r\mu] \frac{f_{cc}}{10} & \varepsilon_{cc} \leq \varepsilon_c < 11\varepsilon_{cc} \\ r\mu f_{cc} & 11\varepsilon_{cc} \leq \varepsilon_c \leq 0.03 \end{cases} \quad (60)$$

where R_2 is a undetermined coefficient given by Eq. (55), and r is defined as the material degradation factor, which is introduced by Ellobody and Young (2006), based on the experimental investigation, to account for the effect of diverse concrete strengths. The parameter r can be taken as 1.0 for concrete with cube strength (f_{cu}) of 30 Mpa and 0.5 for concrete with cube strength (f_{cu}) of larger than or equal to 100 Mpa, respectively. Linear interpolation may be adopted to confirm the value of r for strength between 30 and 100 Mpa. μ is defined as the softening behavior reduction factor and depends on the comprehensive index as nominal confinement factor θ defined by the section above as shown in Eq. (36). The approximate value of μ can be calculated from empirical equations given by experimental data.

Generally, the parameters μ and f_{cl} should be obtained for the sake of completely defining the equivalent uniaxial stress-strain relation. These two parameters apparently depend on comprehensive index as nominal confinement factor θ . Consequently, their appropriate values are ascertained by deducing empirical equations via experimental resultant study (Chang *et al.* 2013, Liew and Xiong 2012, Jiang *et al.* 2008, Peng *et al.* 2011).

Figs. 12(a)-(b) show the values of f_{cl}/θ and μ versus the confinement factor θ for CFDST columns, respectively. From the results of the test data, the empirical equations may be proposed for f_{cl}/θ as follows

$$f_{cl}/\theta = 5.643\theta^2 - 25.635\theta + 31.668 \quad 0.5 \leq \theta \leq 2.5 \quad (61)$$

Due to the limited test data, Eq. (61) is not obtained by a larger scope. Instead, it is formed by a parabola decreasing function connecting the data points at $\theta = 0.5, 2.5$ (Fig. 12(a)). For the parameter μ , two empirical equations may be proposed as follows

$$\mu = \begin{cases} 0.22\theta + 0.78 & 0.5 \leq \theta < 1 \\ 1 & 1 \leq \theta \leq 2.5 \end{cases} \quad (62)$$

in which Eq. (62) is a linear increasing formula passing through the data points at $\theta = 0.5, 1$ and a horizontal line connecting the data points at $\theta = 1, 2.5$ with its terminal point at $\theta = 2.5$ (Fig. 12(b)). The behaviors of CFDST columns are highly influenced by the factor μ . When $\mu = 1$, the axial stress-strain curves do not show a degrading effect. However, when $\mu < 1$, the curves do show a degrading effect. This degrading phenomenon is more prominent with a smaller value of μ .

The damage plasticity model defined in ABAQUS was used for the concrete in the analysis. In the present finite element models, strength enhancement at the state of triaxial loading can be achieved by the definition of the yielding surface with a unique yield function with non-associated flow and a Drucker-Prager hyperbolic flow potential function, and the description of the plastic behaviour comes from the equivalent stress-strain relationship of core concrete in Fig. 10(b). For the concrete in tension, the tension softening behaviour of concrete was defined. And the fracture

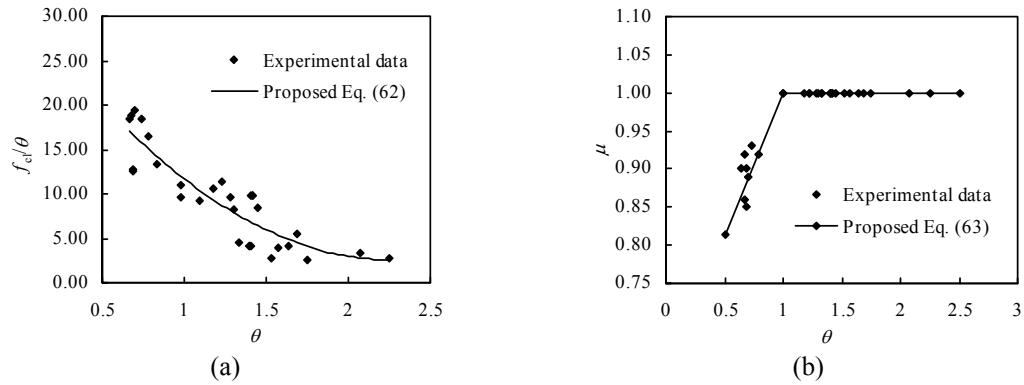


Fig. 12 The relationship curves for CFDST columns. (a) f_{cl}/θ versus θ ; (b) μ versus θ

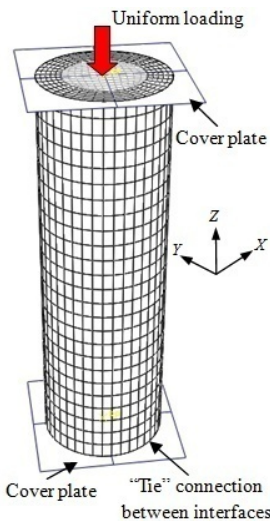


Fig. 13 Boundary condition of short column analytical model

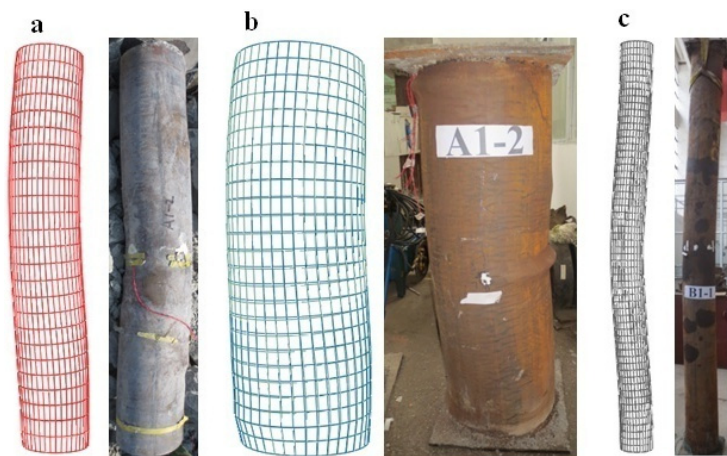


Fig. 14 Comparisons of failure modes. (a) inner specimen A1-2 after split; (b) general specimen A1-2; (c) general specimen B1-1

energy G_f versus the cracking displacement relationship is used to describe the tensile behaviour of concrete.

4.1.2 Finite element type and mesh

Steel tubes of CFDST column are modelled by using 4-node shell elements with reduced integration (S4R), while the sandwiched and core concrete are simulated by 8-node linear brick elements with reduced integration (C3D8R), with three translation degrees of freedom at each node. The mesh for a typical short column is shown in Fig. 13 and a structured mesh technique can be adopted for element partition.

4.1.3 Steel tube-concrete interface model

A surface-to-surface interaction, with a contact pressure-overclosure model in the normal direction, and a penalty function method and Coulomb friction law in the tangential direction

between surfaces of steel tube and core concrete was used for evaluating normal contact force and tangent friction force, respectively.

According to the contact model, the “Hard contact” relation is selected as normal mechanical property. This property can be described as surfaces transmit no contact pressure unless the nodes of the slave surface contact the master surface. There is no limitation on pressure development when surfaces are in contact. Furthermore, the contact surfaces are allowed to separate each other after they have contacted.

According to the Coulomb friction model, the surfaces can transfer the shear stress until the shear stress is greater than the limit static friction force value (τ_{crit}). Afterwards the relative slip is formed between the surfaces, the shear force is taken as a constant. The value of τ_{crit} is dependent on the confinement stress (p) between the surfaces of steel tube and concrete. τ_{crit} can be expressed as

$$\tau_{\text{crit}} = \mu p \geq \tau_{\text{bond}} \quad (63)$$

where μ is the friction coefficient and τ_{bond} is the average surface bond stress.

Selection of the friction coefficient is difficult because there is no standard test procedure to determine it. The friction coefficient μ between steel and concrete is taken as from 0.2 to 0.6 by Baltay and Gjelsvik (1990). According to the existing studies and standards, the friction coefficient used for CFST columns ranged from 0.2 to 0.7, where a constant friction coefficient of 0.25, 0.6, 0.3, 0.2 or 0.3, 0.25, 0.25 and 0.4, 0.4, 0.7 and 0.5 are suggested by Ellobody and Young (2006), Han *et al.* (2007), Espinos *et al.* (2010), Dai and Lam (2010), Hu and Su (2011), Hassanein *et al.* (2013), Chang *et al.* (2013), ACI (2002) and Eurocode 4 (2004), respectively. Thus, in this paper, the friction coefficients of 0.5 based on Chang *et al.* (2013) between inner steel tube and both the sandwiched and the core concrete and 0.25 (Ellobody and Young 2006) between the outer steel tube and the sandwiched concrete are utilized to achieve a quick convergence and to obtain an accurate result.

The geometric property of the contact surfaces is defined by selecting appropriate contact discretization, tracking approach and determination of master and slave surfaces for the contact (ABAQUS standard 2008). Surface-to-surface contact discretization is used in which two of the contact surfaces are defined as master and slave surfaces respectively. In this paper, the steel tube surface was chosen as master surfaces whereas the sandwiched concrete and core concrete surfaces were chosen as slave surfaces. The nodes in the master surface may penetrate into the slave surface. A finite sliding tracking approach can be selected for the contact in view of the actual sliding value between steel and concrete surfaces in CFDST column is relatively small.

4.1.4 Boundary conditions and load application

The cover plate considered herein is employed in the form of an analytical rigid body. The cover plate connects with the steel tube by “Tie” (an interface model in ABAQUS), which ensures the displacements and rotational angles of the contact elements keep the same in the whole loading process. Moreover, the “Hard contact” relation is selected for the cover plate and concrete.

A maximum initial geometrical deflection of $L/1000$ (where L is the length of the specimen) was taken into account for slender columns ($\lambda > 20$) if the overall initial deflection is not provided. Load is simulated by applying displacement instead of directly applying load. Thus, the uniform axial loading in the z -direction is applied statically to the top surface of the cover plate. The load was applied incrementally using the well-known Newton-Raphson incremental-iterative solution method, to determine the response of CFDST subjected to axial compressive load. The response of

CFDST after each step is calculated from the equilibrium equations. The nonlinear geometry parameter (*NLGEOM) was included to deal with the large displacement analysis. The load application for a typical CFDST column is presented in Fig. 13.

4.2 Comparisons with experimental results

Fig. 14 shows the comparison of the predicted and experimental results of the typical specimen A1-2 and B1-1 failure pattern when the load is dropped by 30% after the limit load. From the Figs. 14(a)-(b), it is obvious that the middle side buckling of the specimen typically occur first, and then the buckling also happens on both ends in the loading process. And the buckling of the ends and central position are in the opposite directions. In addition, Fig. 14(c) gives a general view of the slender specimen B1-1 after the test. During the test, the lateral deflection curve was approximately in the shape of a half sine wave.

Typically predicted axial load N versus axial strain ϵ or axial displacement u curves using FE modelling are compared with the measured curves (see Fig. 15). Due to the fact that predicted curves of short columns do not appear to be at the descending stage from the Figs. 15(a)-(g), the

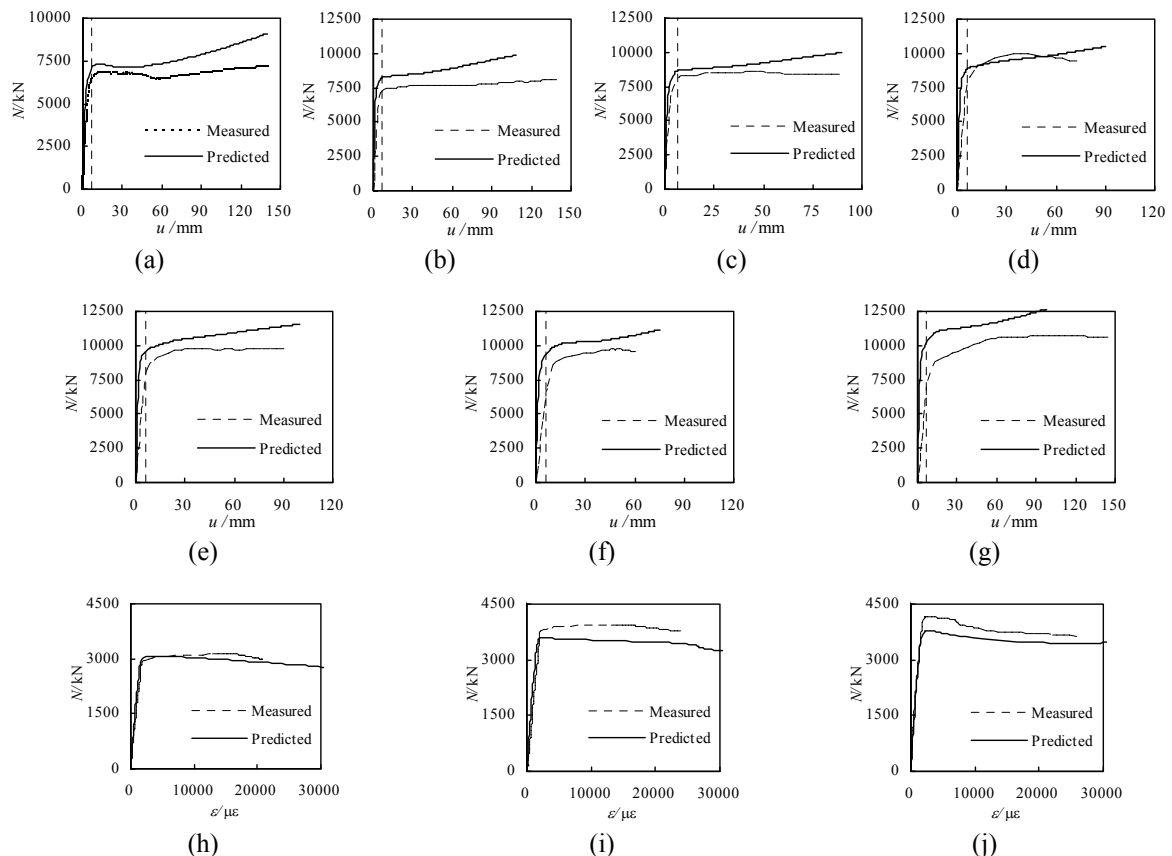


Fig. 15 Comparisons of predicted load versus deformation curves with measured results. (a) Column A-1; (b) Column A1-1; (c) Column A2-1; (d) Column A1-2; (e) Column A2-2; (f) Column A1-3; (g) Column A2-3; (h) Column B-1; (i) Column B1-1; (j) Column B1-2

compressive strength of a concrete filled double steel tubular column is determined to be the stress corresponding to the longitudinal strain of $5000 \mu\epsilon$ based on the value ranges in Ref. (Zhong 2006, Han *et al.* 2008) and the numerical results calculated by Hassanein *et al.* (2013) and Chang *et al.* (2013). That means the intersection of the vertical dotted line and the load-deformation curve calculated by FEM is the predicted bearing capacity value in Fig. 15. It appears that the FE model incorporating the proposed concrete model generally predicts well the complete axial load-deformation curves for the tested CFDST columns. A mean (N_{fe}/N_{ue}) of 0.962 and a COV (coefficient of variation) of 0.002 for members are obtained, as shown in table 1. It can be found that, in general, good agreement is obtained among the FEA, formulas predicted and experimental results.

5. Conclusions

This paper has presented a novel unified design formula, experimental studies and a nonlinear improved finite element model for the analysis of concrete-filled double steel tubular columns under axial compression. An equivalent uniaxial stress-strain relationship for the concrete confined by both the outer and inner steel tube is proposed and then is applied to improve the finite element model for these composite columns. The comparison among the theoretical predictions, the finite element results and the experimental results of the columns with different inner steel ratios and yield strength shows good agreement in predicting the behaviour and strength of the columns. The columns strengths, load-deformation curves and failure modes of the columns have been predicted by using the finite element model and they are generally compared well with the experimental results. The following conclusions can be drawn based on the study about this paper:

- (1) The CFDST columns can provide additional confining effects on the concrete core and lead to different failure mode, stronger bearing capacity and better ductility, as compared to plain CFST columns. Generally, during the axial loading process, both of inner and outer steel tubes have yielded before reaching the ultimate load, which gives full play to the role of steel products. At the same steel ratio, the higher inner tube yield strength, the greater the bearing capacity of the columns. When the steel ratio reaches a certain value, it is not obvious for the improvement of the strength. The presence of the inner steel tube not only can improve the bearing capacity of the columns, but also can increase the stiffness.
- (2) This design formula provides a unified formulation for both the plain concrete filled steel tubular (CFST) and CFDST columns relating to the compressive strength or the stability bearing capacity and a set of design parameters. In addition, the formula is in line with the National code (Chinese Standard 2014).
- (3) The present finite element studies will be a foundation for further extensive parametric analysis on the fundamental mechanic performance of CFDST columns under different stress load at room and elevated temperature with different section forms, and the different material including self-consolidating or lightweight concrete, and some other special type of steel is also possible.

References

ABAQUS standard user's manual (2008), The Abaqus Software is a product of Dassault Systèmes Simulia Corp.; Dassault Systèmes, Version 6.8, Providence, RI, USA.

- ACI (2002), Building Code Requirements for Structural Concrete and Commentary, American Concrete Institute; ACI-318-02, Detroit, MI, USA.
- Baltay, p. and Gjelsvik, A. (1990), "Coefficient of friction for steel on concrete at high normal stress", *J. Mater. Civil Eng., ASCE*, **2**(1), 46-49.
- Chang, X., Ru, Z.L., Zhou, W. and Zhang, Y.B. (2013), "Study on concrete-filled stainless steel-carbon steel tubular (CFST) stub columns under compression", *Thin-Wall. Struct.*, **63**, 125-133.
- Chinese Standard (2014), Technical Code for Concrete Filled Steel Tubular Structures, China Building Industry Press; GB 50936-2014, Beijing, China. [In Chinese]
- Dai, X. and Lam, D. (2010), "Numerical modeling of the axial compressive behaviour of short concrete-filled elliptical steel columns", *J. Constr. Steel Res.*, **66**(7), 931-942.
- Ellobody, E. and Young, B. (2006), "Nonlinear analysis of concrete-filled steel SHS and RHS columns", *Thin-Wall. Struct.*, **44**(8), 919-930.
- Espinos, A., Romero, M.L. and Hospitaler, A. (2010), "Advanced model for predicting the fire response of concrete filled tubular columns", *J. Construct. Steel Res.*, **66**(8-9), 1030-1046.
- Eurocode 4 (2004), Design of composite steel and concrete structures. Part 1.1, General rules and rules for buildings; DD ENV 1994-1-1, British Standards Institution, London, UK.
- Han, L.H., Yao, G.H. and Tao, Z. (2007), "Performance of concrete-filled thin-walled steel tubes under pure torsion", *Thin-Wall. Struct.*, **45**(1), 24-36.
- Han, L.H., Liu, W. and Yang, Y. (2008), "Behaviour of concrete-filled steel tubular stub columns subjected to axially local compression", *J. Constr. Steel Res.*, **64**(4), 377-387.
- Hassanein, M.F., Kharoob, O.F. and Liang, Q.Q. (2013), "Behaviour of circular concrete-filled lean duplex stainless steel-carbon steel tubular short columns", *Eng. Struct.*, **56**, 83-94.
- Hu, H.T. and Su, F.C. (2011), "Nonlinear analysis of short concrete-filled double skin tube columns subjected to axial compressive forces", *Mar. Struct.*, **24**(4), 319-337.
- Huang, H., Han, L.H., Tao, Z. and Zhao, X.L. (2010), "Analytical behaviour of concrete-filled double skin steel tubular (CFDST) stub columns", *J. Constr. Steel Res.*, **66**(4), 542-555.
- Jiang, H., Zuo, J. and Cheng, W.R. (2008), "Experimental study of concrete-filled double steel tubular short columns subjected to axial compression load", *Earthq. Resist. Eng. Retrof.*, **30**(1), 28-35. [In Chinese]
- Li, W., Ren, Q.X., Han, L.H. and Zhao, X.L. (2012), "Behaviour of tapered concrete-filled double skin steel tubular (CFDST) stub columns", *Thin-Wall. Struct.*, **57**, 37-48.
- Liang, Q.Q. (2009), "Performance-based analysis of concrete-filled steel tubular beam-columns. Part I: theory and algorithms", *J. Constr. Steel Res.*, **65**(2), 363-373.
- Liew, J.Y.R. and Xiong, D.X. (2012), "Ultra-high strength concrete filled composite columns for multi-storey building construction", *Adv. Struct. Eng.*, **15**(9), 1487-1504.
- Lin, M.L. and Tsai, K.C. (2001), "Behavior of double-skinned composite steel tubular columns subjected to combined axial and flexural loads", *Proceedings of the First International Conference on Steel & Composite Structures*, Busan, Korea, June.
- Mander, J.B., Priestley, M.J. and Park, R. (1988), "Theoretical stress-strain model for confined concrete", *J. Struct. Eng.-ASCE*, **114**(8), 1804-1826.
- Martinez, S., Nilson, H.N. and Slate, F.O. (1984), "Spirally reinforced high-strength concrete columns", *ACI Struct. J.*, **81**(5), 431-442.
- Peng, Y.Y., Tan, K.F. and Yao, Y. (2011), "Mechanical properties of duplex steel tubular high strength concrete short columns", *J. Southwest Univ. Sci. Technol.*, **26**(2), 105-109. [In Chinese]
- Richart, F.E., Brandzaeg, A. and Brown, R.L. (1928), "A study of the failure of concrete under combined compressive stresses", University of Illinois Engineering Experimental Station; Bull., 185, Champaign, IL, USA.
- Romero, M.L., Espinos, A., Portolés, J.M., Hospitaler, A. and Ibañez, C. (2015), "Slender double-tube ultra-high strength concrete-filled tubular columns under ambient temperature and fire", *Eng. Struct.*, **99**(15), 536-545.
- Saenz, L.P. (1964), "Discussion of paper by Desai P, Krishnan S. equation for stress-strain curve of concrete", *J. Am. Concrete Inst.*, **61**(7), 1229-1235.

- Sakino, K., Nakahara, H., Morino, S. and Nishiyama, I. (2004), "Behavior of centrally loaded concrete-filled steel-tube short columns", *J. Struct. Eng.-ASCE*, **130**(2), 180-188.
- Wei, H., Wang, H.J., Hasegawa, A., Shioi, Y., Iwasaki, S. and Miyamoto, Y. (2005), "Study on strength of reinforced concrete filled circular steel tubular columns", *Struct. Eng. Mech., Int. J.*, **19**(6), 653-677.
- Xiamuxi, A. and Hasegawa, A. (2012), "A study on axial compressive behaviors of reinforced concrete filled tubular steel columns", *J. Constr. Steel Res.*, **76**, 144-154.
- Yagishita, F., Kitoh, H., Sugimoto, M., Tanihira, T. and Sonoda, K. (2000), "Double-skin composite tubular columns subjected cyclic horizontal force and constant axial force", *Proceedings of the 6th ASCCS Conference*, Los Angeles, CA, USA, March.
- Yu, M., Zha, X.X., Ye, J.Q. and Li, Y.T. (2013), "A unified formulation for circle and polygon concrete-filled steel tube columns under axial compression", *Eng. Struct.*, **49**, 1-10.
- Zhong, S.T. (2006), *Concrete-filled Steel Tube United Theory-Research and Application*, Tsinghua University Press, Beijing, China. [In Chinese]
- Гвоздев, А.А. (1949), *Расчет несущей способности конструкций по методу предельного равновесия*, Госстройиздат, Москва, Россия.

DL

Nomenclature

A_c	Cross-sectional area of concrete
$A_{c,1}, A_{c,2}$	Cross-sectional area of sandwich and core concrete, respectively
$A_s, A_{s,1}$	Cross-sectional area of outer and inner steel tube, respectively
A_{ce}	Nominal cross-sectional area of concrete, $A_{ce} = \pi/4(D_o - 2t_o)^2$
A_{sc}	Cross-sectional area of CFDST column
A_i	Cross-sectional area of inner steel tube
D_o	Outer dimension of outer circular steel tube
D_i	Outer diameter of inner circular steel tube
E_{sc}, I_{sc}	Composite bending modulus and moment of inertia, respectively
f_{sc}	Composite axial strength
f_s	Yield strength of steel tube
f_{cu}	Concrete cube strength
f_{ck}	Concrete compressive strength ($f_{ck} = 0.67 f_{cu}$ for normal strength concrete)
f_{yi}, f_{yo}	Yield strength of inner and outer steel tube, respectively
f_{si}	Ultimate strength of inner steel tube
f_{so}	Ultimate strength of outer steel tube
L	Column height
N, N_u	Axial compressive strength and stability bearing capacity, respectively
N_{ue}	Measured experimental ultimate strength of CFDST column
N_{cal}	Formulas predicted ultimate strength of CFDST column
N_{fe}	FEA predicted ultimate strength of CFDST column
p_1, p_2, p_3	Lateral pressure of the interface between concrete and steel tube, respectively
r_1, r_3	Outside radius of outer and inner steel tube, respectively
r_2, r_4	Radius of the interface between sandwich concrete and outer steel tube, core concrete and inner steel tube, respectively
t_o, t_i	Wall thickness of outer and inner steel tube, respectively
ν_c	Poisson's ratio of concrete
ρ_i	Steel ratio of inner tube
μ_s	Poisson's ratio of steel